Contribution to "Diamond Jubilee of RCA"

Gaia Pupillo*, Liliana Mou, Simone Manenti*, Flavia Groppi, Juan Esposito and Ferid Haddad

Nuclear data for light charged particle induced production of emerging medical radionuclides

https://doi.org/10.1515/ract-2022-0011
Received January 14, 2022; accepted April 14, 2022;
published online May 13, 2022

Abstract: Whatever the radionuclide to be used in nuclear medicine, it is essential to know the expected yield during the production process, but also of all the possible radionuclidic impurities coproduced, that can have an impact on the product final quality, as well as in the related waste management. The availability of the majority of emerging radioisotopes, including the theranostic ones or pairs, is mainly limited by the fact that, for most of them, the optimal production route still needs to be strengthened if not defined in some cases. The aim of this work is to present a review on the charged particle induced nuclear cross sections to produce some emerging radionuclides for medical applications to show that all types of projectiles should be considered in the quest of producing medical radionuclides. An accurate analysis of the production routes is presented for some radionuclides (^{67}Cu, ^{47}Sc, ^{89}Zr, ^{103}Pd, ^{186g}Re, ^{97}Ru, ^{211}At) chosen as examples to highlight (i) how the quality of the final product strongly depends on the chosen target/projectile/energy parameters set, (ii) how deuteron production routes may sometimes be more effective than the proton ones or lead to a different impurity profile and (iii) how α-particle beams may allow to bypass the limitations occurring when using Z = 1 beams. An overview of possible advantages and drawbacks of the cited production routes and of potential cross sections that still need to be measured, is also reported.

Keywords: charged-particles induced reactions; medical radionuclides; particle accelerators; production cross sections.

1 Introduction

1.1 Radionuclides in nuclear medicine

Nuclear Medicine is a medical field that uses radionuclides both for diagnosis and therapy. The physical characteristics of radioactive decay of radionuclides determine their use in nuclear medicine [1–3]. In most cases, radionuclides must be labelled to a vector molecule, forming what is commonly called a radiopharmaceutical. The vector molecule allows to efficiently target a dedicated cell type, due to its high affinity for it, or for a specific function of the human organ. In general, radionuclides employed in nuclear medicine both for diagnostic and therapeutic purposes, should meet the following specific requirements:

- appropriate physical properties for the selected application, in terms of half-life ($T_{1/2}$), decay mode and radiation emission energy;
- suitable chemical properties to allow their labelling to a vector molecule with high radiochemical yields through the labelling process;
- ability to deliver an appropriate radiation dose to the target tissue, sufficient to accomplish the intended clinical duty (diagnosis or therapy), but without causing damages to the patient;
- an appropriate purity, as the vector molecule can be expensive or the number of targeted sites limited;
- a reasonable price.

A new frontier of nuclear medicine is the so-called "theranostic approach" that combines therapy and

*Corresponding authors: **Gaia Pupillo**, Istituto Nazionale di Fisica Nucleare, Laboratori Nazionali di Legnaro (INFN-LNL), Viale dell'Università 2, 35020 Legnaro (PD), Italy,
E-mail: gaia.pupillo@lnl.infn.it; and **Simone Manenti**, Department of Physics, University of Milan, Via Celoria 16, I-20133, Milano, Italy; and Department of Physics, Laboratorio Acceleratori e Superconduttività Applicata (LASA), University of Milan and INFN-Milan, Via F.lli Cervi 201, I-20090, Segrate, Italy, E-mail: simone.manenti@unimi.it
Liliana Mou and Juan Esposito, Istituto Nazionale di Fisica Nucleare, Laboratori Nazionali di Legnaro (INFN-LNL), Viale dell'Università 2, 35020 Legnaro (PD), Italy
Flavia Groppi, Department of Physics, University of Milan, Via Celoria 16, I-20133, Milano, Italy; and Department of Physics, Laboratorio Acceleratori e Superconduttività Applicata (LASA), University of Milan and INFN-Milan, Via F.lli Cervi 201, I-20090, Segrate, Italy
Ferid Haddad, GIP ARRONAX, 1 Rue Aronax, 44800 Saint Herblain, France; and Laboratoire SUBATECH, CNRS/IN2P3, IMT Atlantique, Nantes Université, 4, rue Alfred Kastler, 44307 Nantes, France

diagnosis stages (preferentially PET imaging that can give a quantitative dosimetry) [4], and which includes a single radiopharmaceutical that:

- has both diagnostic and therapeutic properties, i.e. a bioactive molecule labelled with an isotope whose radiation decay pattern is suitable both for diagnosis and therapy, such as ^{47}Sc, ^{67}Cu, ^{67}Ga, ^{111}In, ^{117m}Sn ^{123}I, ^{131}I, ^{153}Sm, ^{177}Lu, ^{186}Re, ^{213}Bi, etc.; as previously noted, the use of gamma-emitters instead of positron-emitters is recently attracting considerable interest [4];
- can be labelled with different radioisotopes of the same element, one being utilized for diagnosis while the other one for therapy, such as $^{43/44}$Sc/^{47}Sc, $^{61/64}$Cu/^{67}Cu, ^{68}Ga/^{67}Ga, ^{86}Y/^{90}Y, ^{124}I/^{131}I, the terbium family $^{149/152}$Tb/$^{155/161}$Tb, etc. [5];
- can be labelled with different isotopes each belonging to a different element but having similar chemical properties (surrogate pair), where one radionuclide is utilized for diagnosis and the other for therapy, such as ^{68}Ga/^{177}Lu, ^{68}Ga/therapeutic lanthanide, etc.

The theranostic approach allows for collecting pre-therapy information with low-dose diagnostic imaging, aimed at optimizing the following high-dose therapeutic administration to the patient [6]. This strategy is getting closer to the realization of personalized medicine, in which low-dose molecular imaging performed with SPECT/CT or PET/CT is a necessary step to provide preliminary information about biodistribution, dosimetry on the tumor and limiting or critical organs or tissues, and the maximum tolerable dose [7].

Whatever the radionuclide to be used in nuclear medicine, it is thus essential to get knowledge of the possible presence of coproduced radionuclidic impurities that can have an impact on the final product quality and in the waste management during the production process or in the use at the hospital. Moreover, the availability of the majority of theranostic radionuclides is mainly limited by the fact that most of them are currently emerging and the optimal production route still needs to be improved or defined [8, 9].

1.2 The use of accelerators for emerging medical radionuclides production

Most of the radionuclides used in nuclear medicine are artificially produced by using either nuclear reactors or accelerators delivering charged particle beams or inducing a γ-irradiation. This work is focused on light-charged particles induced reactions, even if there is an increasing interest on photo-production as for example for ^{47}Sc, ^{67}Cu, etc. [10–12].

In order to select the optimal way to produce a given radionuclide, it is mandatory to explore all possible nuclear reaction routes and thus to measure the nuclear cross sections for the concerned radioisotope, as well as of related main contaminants. Among the possible production routes, proton or light-charged particles (e.g. deuteron, ^{3}He and ^{4}He) are of great potential, mainly for positron emitters and some therapeutic radionuclides [13, 14]. In recent years, high energy (70 MeV) and multi particle accelerators have been made available from accelerators' manufacturers. This allows to widen the range of possible nuclear reaction routes which may be explored and radionuclides that may be thus produced (e.g. ^{211}At or ^{82}Sr, ^{68}Ge, etc.). Examples in Europe are the ARRONAX facility [15] and the SPES cyclotron used in the LARAMED project [16].

1.3 The importance of accurate nuclear cross section determination and thick target yields (TTY) measurements in medical radionuclides production

By definition, the cross section σ(E) is the probability of a specific nuclear reaction to occur at the given energy E, i.e. the interaction probability of one bombarding particle and one target atom. This quantity is required to calculate the production yield of the radionuclide of interest. Indeed, the resulting activity at the End Of Bombardment (TTY_{EOB}) of a given radionuclide, produced by a particle beam hitting a thick target, which also depends on the irradiation time t_{IRR} and the decay constant λ [s^{-1}], is calculated considering the following formula [3, 17]:

$$TTY_{EOB} = \frac{N_A N_b}{A_T}\left(1 - e^{-\lambda t_{irr}}\right)\int_{E_{out}}^{E_{in}} \sigma(E)\frac{dE}{S_T(E)} \qquad (1)$$

where N_A is the Avogadro constant [mol^{-1}], N_b is the number of bombarding particles [s^{-1}], A_T is the atomic weight of the target material [$g{\cdot}mol^{-1}$] and $S_T(E)$ is the mass stopping power of the particle beam through the target material at the energy E, expressed as dE/d(ρx). The term $(1 - e^{-\lambda t_{irr}})$ is the so-called saturation factor (SF) that takes into account both the production of nuclei due to the considered nuclear reaction and the decay of nuclei that have already been produced. In a thick

target, the impinging projectile energy decreases as it penetrates into the target thickness, thus the energy variation against target thickness, and the related variation of the cross section versus energy, must be considered.

The parameters that have an impact on the production yield (TTY) are the beam intensity, the irradiation time and the beam energy range: the beam intensity is limited by the maximum beam current available by the accelerator and also by the thermal-mechanical main features associated to the targetry; the irradiation time can be increased, keeping in mind that the SF trend keeps linear until the irradiation time remains below one $T_{1/2}$; the projectile energy range can be adapted to exploit the maximum cross section value, considering the limitation due to the coproduction of contaminants, by adjusting the incident energy and the target thickness. The presence of contaminants, especially radionuclides with close to or longer half-life than the desired radionuclide, affects the purity of the final product and may cause a dose increase to the patient.

To limit as much as possible the reaction routes which may be opened, and thus the coproduction of undesired radionuclides, it is often necessary to use expensive isotopically enriched materials. Even considering the ideal case of a fully monoisotopic target, it is foreseen the coproduction of isotopic contaminants, depending upon the beam energy range chosen. A good knowledge of production cross sections for all the occurring nuclear reaction routes is therefore a key point that has to be carefully considered. The production cross section of the concerned radionuclide, as well as those of main contaminants, the optimal irradiation parameters may be at last selected, i.e. the irradiation time and beam energy range, in order to ensure the achievement of the best final product purity given by the Specific Activity A_S [Bq·g^{-1}], the Radio Nuclidic Purity RNP [%] and the Isotopic Purity IP [%] parameters [2, 18].

1.3.1 Experimental details on a nuclear cross section measurement

The use of a single thin homogeneous target foil, followed by a precise Faraday cup to measure the hitting beam current, is the best method to obtain an accurate measurement of a specific nuclear cross section. However, due to the limited access to beam time it is often preferred to use the well-known stacked-foils technique that allows, by the simultaneous bombardment of patterns composed of target and degrader foils, to get the experimental determination of some cross section values at different beam energies during the same irradiation run. In order to control the beam energy loss through the target stack, it is desirable to insert in the structure at least two monitor foils of an element for which the production cross section of a given reaction route is well known and that acts as a reference. Particular attention has also to be paid to the material used in the stack both for degrader and monitor foils, since the recoil effect, i.e. when some atoms jump out of one foil and are trapped in the following one, may also cause some additional interferences in the γ-spectrometry acquisitions.

In addition to the aforementioned parameters that have to be taken under control for a precise nuclear cross section measurement, it is important to remind the role of the target thickness (homogeneity and purity), the beam stability during the irradiation run and the beam energy precision (the possibility to use a tunable energy accelerator is favourable), the detector calibration (energy and efficiency) and the possible interferences in the emitted γ-lines or in the decay relations among metastable/ground state or parent/daughter radionuclides.

1.3.2 Theoretical aspects on nuclear cross sections assessment

Theoretical description of nuclear reactions, occurring below 100 MeV/amu, imply many different interaction processes, such as the compound-nucleus reaction, the direct nuclear reaction, and the pre-equilibrium nuclear reactions [19]. Several nuclear reaction codes are available that include models that implement these different nuclear reaction mechanisms between a target nucleus and a hitting particle. The most used ones are TALYS [20, 21], EMPIRE [22], FLUKA [23, 24] and MCNPX [25]. They are usually exploited to estimate the trend contributions for those nuclear reaction routes, whose cross sections data are not measured yet. The IAEA tool ISOTOPIA [26] is instead based on the IAEA data as well as on the TENDL library [27], a nuclear database built on the TALYS code. TALYS is used to simulate nuclear reactions involving protons, neutrons, deuterons, photons, tritons, ^{3}He and α-particles, in the 1 keV to 200 MeV energy range and covers target nuclides of mass 12 and heavier. TALYS includes a large number of different models and some of them are invoked in calculation by default. Concerning compound reaction contributions, TALYS 1.9, the last version available to date, performs default calculations in the Hauser–Feshbach approach with Moldauer width fluctuation corrections. Koning and Delaroche local parametrization for the optical model is used with different models to take into account direct reaction contributions: Distorted-Wave Born Approximation (DWBA) Coupled-channels (rotational and vibrational approaches). Since

TALYS has been used in many works to benchmark the experimental determination of nuclear cross sections for many radionuclides of interest in medicine, we mainly refer to this code in this review study. We focused on TENDL-2021 which is based on the last version of the TALYS code. However, in some cases the TENDL-2021 cross sections are different from the earlier versions (and in few cases less in agreement with available data), underlining the need of additional work, both for new experimental data to constrain the code and in the optimal identification of the TALYS parameters that better describe the nuclear reactions for this kind of applications [28].

2 Charged-particles induced reactions

Nowadays, most accelerator-based radionuclides are produced using proton beams. This is mostly linked to the fact that there is a large installed network of low-energy cyclotrons, often called Small Medical Cyclotron (SMC) [29], and that protons can be accelerated as negative ions that are extracted with nearly 100% efficiency using stripper foils. Alpha particles may instead only be accelerated as positive ions and the extraction process is more challenging. With the larger availability of both medium and high energy accelerators, new linear accelerator like SPIRAL2 [30] or the one available at SOREQ [31] providing p, d, α-particles beams with mA intensities, and multi-particle cyclotrons allowing access to high energy deuterons and α particles beams, the production routes for established as well as emerging radionuclides may thus be re-investigated. In all cases, by changing the projectile type and/or its energy and/or the target material, it is possible to adapt the production yield and the profile of contaminants [32]. In the following examples, we will present some cases showing that:

- the quality of the final product strongly depends on the chosen target/projectile/energy parameters set (^{67}Cu and ^{47}Sc cases);
- the deuterons-based production route may sometimes lead to a different impurity profile (^{67}Cu and ^{89}Zr examples) or be more effective than the protons-based one (^{103}Pd and ^{186}Re case). This latter property is basically due to the more complex deuteron-induced interaction process with respect to the proton one (i.e. involving the breakup mechanism, direct reaction stripping, and pre-equilibrium and compound-nucleus) that have been studied in different former works which details may be found in [33–35]. Because of the weak binding energy of deuterons, B_d = 2.224 MeV, a more complex interaction process indeed occurs, that involves different reaction routes started by neutrons and protons following the deuteron breakup that enhance the production route. Moreover, a reliable description of the deuteron-nucleus interaction is a good test for the quality of the reaction mechanism modeling, as well as the evaluation of the nuclear data;
- α-particle beams may allow to bypass the limitations occurring when using proton beams (^{97}Ru and ^{211}At examples). A complete description of potential of alpha beam can be found in [14].

Table 1 shows the decay characteristics, extracted from the NuDat 3.0 database [36], of the medical radionuclides considered in this review. When available, the recommended IAEA curves [37–39] will be used instead of the available data sets [40] for simplicity and readability.

2.1 ^{67}Cu

^{67}Cu has a half-life of 61.83 h and it is emitting β^- and γ radiation [36]. The energy of β^- particles is appropriate for therapy (141 keV as mean energy, corresponding to about

Table 1: Main decay data of the radionuclides of interest [36].

RN	Half-life	Main γ-ray energy, intensity [keV] (%)	Mean β^+ energy, intensity [keV] (%)	Mean β^-energy, intensity [keV] (%)	Auger and IC electrons	Main α-particle energy, intensity [keV] (%)
^{67}Cu	61.83 h	184.577 (48.7)	–	141 (100)	Yes	
^{47}Sc	3.3492 d	159.381 (68.3)		162 (100)	Yes	
^{89}Zr	78.41 h	909.15 (99.04)	396 (22.74)		Yes	
^{103}Pd	16.991 d				Yes	
^{186g}Re	3.7183 d	137.157 (9.47)		346.7 (92.59)	Yes	
^{97}Ru	2.83 d	215.70 (85.62)			Yes	
		324.49 (10.79)				
^{211}At	7.214 h	687.0 (0.261)			Yes	5869.5 (41.8)

200–300 μm range in soft tissue), while the 185 keV photons are suitable for pre-therapy low dose imaging (SPECT or SPECT/CT). These physical characteristics allow the use of ^{67}Cu for both therapy and associated diagnostic applications, thus making ^{67}Cu a promising theranostic radionuclide. It can be also used as a therapeutic counterpart of the ^{64}Cu (12.7 h half-life and β^-/β^+ emitter), a PET radionuclide [5, 41, 42]. Production techniques for ^{64}Cu are well known and are usually based on the ^{64}Ni(p,n)^{64}Cu and ^{64}Ni(d,2n)^{64}Cu reactions routes [43], even if there are other possibilities [43, 44].

The use of ^{67}Cu has been prevented by the lack of regular availability in enough amounts for preclinical and clinical studies, although it is possible to produce it through many production routes [9, 45, 46]. There is currently not a clear consensus about the best nuclear reaction route to be used for a massive production, due to the impact of the coproduced isotopic ^{64}Cu that occurs with some specific routes [47]. Indeed, the presence of the ^{64}Cu annihilation photons affects the total dose received by the patient and the staff, while the emitted Auger electrons, the positron and the electrons release their energy close to the decay point, adding their contribution to the dose in tissues.

Nuclear data are therefore important to help in defining benefits and drawbacks associated with each of these production routes. Among the feasible ones are the following:

- ^{68}Zn(p,2p): this production method has quite a low cross section (maximum value of around 10 mb) [40] and requires intermediate energy proton-beams (30 < E < 100 MeV), although it can be exploited also at higher energies [48–53]. In order to limit the coproduction of other Cu-radionuclides, which directly affects the radionuclidic purity of the final product, the use of enriched ^{68}Zn targets is mandatory, as well as the recycling of the target material to make this production route affordable. Among the variety of radionuclides produced during the bombardment of a zinc target, ^{67}Ga (half-life 3.2617 d) is particularly relevant: it presents the same γ-lines of ^{67}Cu since they both decay into ^{67}Zn [36]. Moreover, they have a similar half-life, and therefore it is not possible to infer the precise activity determination of one radionuclide waiting for the decay of the other one. For these reasons a radiochemical procedure, aimed at the separation of copper from gallium elements, is thus mandatory to obtain a precise cross section for ^{67}Cu production [49, 54]. The separation procedure, as well as the use of different target materials (natural or enriched), selected monitor reactions or not up-to-date decay data, could explain the large discrepancies of the published data. The measurement carried out at the ARRONAX facility led to an estimated difference on the ^{67}Cu production yield of up to 15% in the 70–35 MeV energy range [54]. This difference has a direct impact on the planning of sustainable production of ^{67}Cu for medical purposes. It should also be outlined that with this production route a large amount of ^{64}Cu is coproduced, as indicated by the ^{68}Zn(p,x)^{64}Cu cross section recommended by the IAEA up to 100 MeV [37]. ^{64}Cu can be limited in the final product by waiting for its decay up to the desired value of the ^{67}Cu radionuclidic purity, however loosing part of the ^{67}Cu activity.
- ^{70}Zn(p,α): this nuclear reaction, already measured up to 35 MeV by Levkovskij (1991) [50] and Kastleiner et al. (1999) [55], has a maximum cross section value of 15 mb at about 15 MeV. This production route can allow the supply of pure ^{67}Cu as there is no coproduction of ^{64}Cu below E_{thr} = 23.8 MeV (threshold energy associated with ^{64}Cu production). Considering the low cross section value this production route provides quite a low yield, i.e. 5.75 MBq/μAh for the 30–10 MeV energy range (corresponding to a 1.79 mm thick target of 100% enriched ^{70}Zn). Also in this case, enriched target material and recycling are mandatory.
- ^{70}Zn(p,x): The use of ^{70}Zn targets at proton energies higher than 35 MeV allows to increase the ^{67}Cu yield (Figure 1 left), limiting the ^{64}Cu coproduction in comparison to the use of ^{68}Zn targets [56]. The ^{67}Cu production cross section reaches a value around 22 mb at 70 MeV, thus it is almost a double value than the recommended cross section by the IAEA, based on ^{68}Zn target. In addition to that, the ^{64}Cu coproduction occurring with ^{70}Zn targets shows a decreasing trend versus the increasing energy, while the opposite trend can be noted when using ^{68}Zn targets (Figure 1 right). TENDL library values [27] seem to overestimate the ^{70}Zn(p,x)^{67}Cu reaction, as well as the ^{68}Zn(p,2p)^{67}Cu cross section (Figure 1 left). On the other hand, TENDL results of the ^{68}Zn(p,x)^{64}Cu cross section slightly underestimate IAEA recommended values and show an energy shift of about 5 MeV for the peak below 30 MeV (Figure 1 right); the trend of the ^{70}Zn(p,x)^{67}Cu cross section is well described by the TENDL-data, but there is an underestimation of the experimental values by about a factor of 2.
- ^{70}Zn(d,x): this nuclear reaction has already been measured in 2012 [57] and in 2021 [58] up to 29 MeV. From the most recent data it was possible to identify the cross section peak value associated with this nuclear reaction (about 30 mb at 23 MeV). The comparison

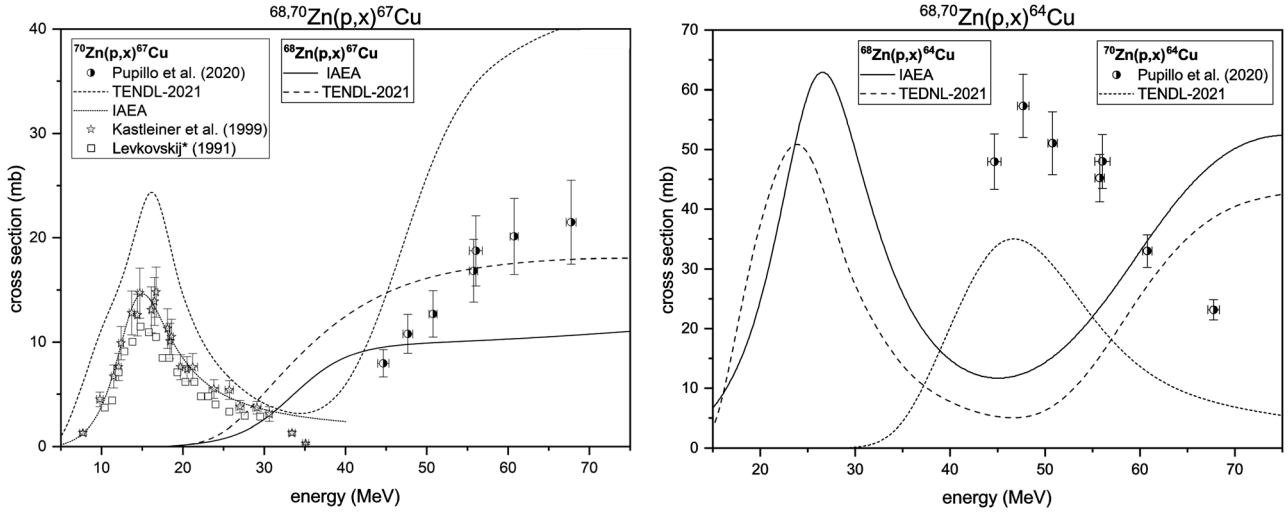

Figure 1: ^{67}Cu (left) and ^{64}Cu (right) production cross sections induced by proton-beams on ^{68}Zn and ^{70}Zn targets.

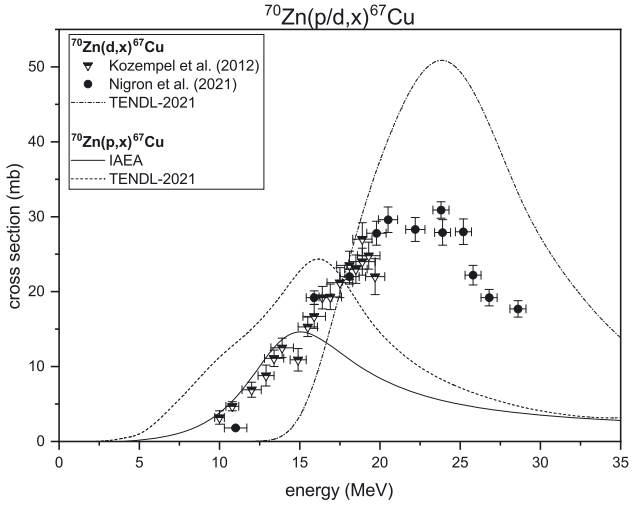

Figure 2: ^{67}Cu production cross sections induced by deuteron and proton beams on ^{70}Zn targets.

between the cross sections data obtained with ^{70}Zn as target material for proton or deuteron beams (Figure 2) shows that the deuteron production route is more efficient than the one using protons. Furthermore, since the threshold associated with ^{64}Cu production is 26.5 MeV, this isotope is not produced in significant amount up to 30 MeV, allowing for a "pure" ^{67}Cu production. The preferred energy range through this route is thus 16–26 MeV, that corresponds to a ^{70}Zn thickness of 576 μm. Considering this energy range, 1 μA beam intensity, 1 h of irradiation time, and a target purity of 97.5%, the estimated production yield is 6.2 MBq [58].

– ^{64}Ni(α,p): this nuclear reaction has been measured since the 1960s up to 50 MeV [50, 59–62] and it presents the maximum value of about 38 mb at 22 MeV. Since the threshold for ^{64}Cu production is 23.7 MeV, this radioisotope is not produced in large amount up to 30 MeV allowing, also in this case, a "pure" production of ^{67}Cu [63]. The main advantage of this production route is the fact that enriched ^{64}Ni target (natural abundance equal to 0.9255%) is well mastered as it is the target used for ^{64}Cu production. A pure ^{67}Cu production requires the use of enriched ^{64}Ni and recycling, making the enrichment level of the target material a crucial aspect (currently it is commercially available with an enrichment level >99%).

To compare the charged-particles induced nuclear reactions, Table 2 presents the ^{67}Cu (and ^{64}Cu) production yields calculated using the IAEA tool ISOTOPIA [26], assuming 100% enriched materials and the same irradiation conditions (^{67}Cu SF = 24%, ^{64}Cu SF = 73%) considering proton, deuteron and α-beams on ^{70}Zn, ^{68}Zn, and ^{64}Ni targets [61].

The values reported in Table 2 show that with a hypothetical fully enriched target material ($^{68/70}$Zn or ^{64}Ni) the

Table 2: ^{67}Cu and ^{64}Cu production yields obtained by using proton, deuteron and α-beams on ^{70}Zn, ^{68}Zn, and ^{64}Ni enriched target materials assuming I = 30 μA and T_{irr} = 24 h.

Beam	Target	Energy range (MeV)	Thickness (mm)	^{67}Cu at EOB (GBq)	^{64}Cu at EOB (GBq)
Protons	^{70}Zn	25–10	1.22	3.0	–
	^{68}Zn	70–35	6.43	17.5	150
	^{70}Zn	68–45	4.61	22.2	140
Deuterons	^{70}Zn	26–13	0.68	4.3	–
Alpha	^{64}Ni	30–0	0.15	1.0	–

most convenient route to obtain ^{67}Cu (without ^{64}Cu coproduction) is by using deuteron beams and ^{70}Zn targets. The final ^{67}Cu quality using this route will be close to that obtained by photo-production [64, 65]. If some ^{64}Cu coproduction is acceptable for clinical application, the ^{68}Zn(p,2p)^{67}Cu reaction seems to be a better option since it provides a larger ^{67}Cu yield in comparison with the ^{70}Zn(d,x)^{67}Cu route mostly because more intense proton beams can be available (hundreds of μA as compared to tens of μA for deuterons). With the same motivation, also the high-energy ^{70}Zn(p,x)^{67}Cu route seems to be interesting. The α-beam production route may benefit soon from the newly available multiparticle 30 MeV accelerators providing tens of μA. The first two machines have been installed in Europe (Jülich and Warsaw) and some others are available in Japan. In the future, linear accelerators that can provide very intense deuteron and α-beam (mA range) are soon foreseen, however in this case the major challenge will be the design of specific targets able to withstand such high currents.

2.2 ^{47}Sc

^{47}Sc (half-life 3.3492 d) is one of the radionuclides of interest in theranostic applications thanks to its β^- and γ-radiation (β^- mean energy 162 keV, 100% intensity; E_γ = 159.381 keV, 68.3% intensity) which makes it suitable for both therapeutic and diagnostic purposes [41, 42]. The interest in ^{47}Sc is also due to the possibility to pair it with a β^+ emitter isotope, such as ^{44g}Sc and ^{43}Sc, allowing to carry out also PET imaging [66]. ^{47}Sc can be produced via different nuclear reaction routes by using cyclotrons, nuclear reactors, and electron linear accelerators [5]; moreover, ^{47}Sc may be produced either directly or by the decay of its parent radionuclide, ^{47}Ca, as shown in Table 3. Particular care must be paid to the other Sc-isotopes produced during irradiation, since they cannot be chemically separated from ^{47}Sc. Among the Sc-isotopic contaminants, the most critical one is ^{46}Sc, due to its long half-life (half-life 83.79 d) and γ emissions (889.277 keV with 99.9840% intensity and 1120.545 keV with 99.9870% intensity).

Considering the proton induced-reactions, the:

- ^{nat}Ti(p,x)^{47}Sc cross section has been widely studied by many research groups, but no energy range has been found in which the ^{47}Sc is produced without ^{46}Sc. Considering the composition of ^{nat}Ti (natural abundances: ^{50}Ti 5.18%, ^{49}Ti 5.41%, ^{48}Ti 73.72%, ^{47}Ti 7.44%, and ^{46}Ti 8.25%) it is not possible to extract from the whole cross sections the contribution of each titanium isotope to the production of the specific radionuclides of interest. Since no data are available for the ^{49}Ti(p,x)^{47}Sc cross section and only a few data sets are published for the ^{50}Ti(p,x)^{47}Sc [45] and the ^{48}Ti(p,2p)^{47}Sc [50, 67, 68] reactions, both studied up to 85 MeV, it will be desirable to add new experimental data in order to evaluate if one of these production routes can be competitive.
- ^{48}Ca(p,2n)^{47}Sc excitation function was measured in 2019 up to 30 MeV [69] reaching a value of 1100 mb at about 18 MeV. However, it must be taken into account that, despite the large cross section value, the natural abundance of ^{48}Ca is only 0.187%, thus making this production route feasible with highly-enriched targets only (enrichment levels available up to 97%), that are anyway very expensive (recycling is mandatory).
- ^{nat}V(p,x)^{47}Sc cross section has been measured by many authors [28, 50, 70–74] up to 200 MeV, reaching a

Table 3: Direct and indirect reactions to produce ^{47}Sc with the nuclear reactions induced by charged particles or neutrons.

	Target	Particle accelerator			Nuclear reactor
		p	d	α	n
Direct reactions	Ti	^{50}Ti(p,α)^{47}Sc	^{50}Ti(d,αn)^{47}Sc		^{47}Ti(n,p)^{47}Sc (fast neutrons)
		^{49}Ti(p,2pn)^{47}Sc	^{49}Ti(d,α)^{47}Sc		
		^{48}Ti(p,2p)^{47}Sc	^{48}Ti(d,2pn)^{47}Sc		
			^{47}Ti(d,2p)^{47}Sc		
	Ca	^{48}Ca(p,2n)^{47}Sc	^{48}Ca(d,3n)^{47}Sc	^{44}Ca(α,p)^{47}Sc	
			^{46}Ca(d,n)^{47}Sc		
	V	^{51}V(p,αp)^{47}Sc	^{51}V(d,x)^{47}Sc		
Indirect reactions	Ti	^{50}Ti(p,3pn)^{47}Ca→^{47}Sc	^{50}Ti(d,αp)^{47}Ca→^{47}Sc		
		^{49}Ti(p,3p)^{47}Ca→^{47}Sc			
	V	^{51}V(p,x)^{47}Ca→^{47}Sc	^{51}V(d,x)^{47}Ca→^{47}Sc		
	Ca	^{48}Ca(p,pn)^{47}Ca→^{47}Sc	^{48}Ca(d,p2n)^{47}Ca→^{47}Sc		^{46}Ca(n,γ)^{47}Ca→^{47}Sc (thermal neutrons)
			^{46}Ca(d,p)^{47}Ca→^{47}Sc		

maximum value of about 12 mb at 34 MeV and for energies higher than 80 MeV. A recent work reported new experimental data for ^{47}Sc and contaminants coproduction using ^{nat}V targets, compared with theoretical estimations obtained by varying the level densities using the TALYS code [28]. Considering ^{nat}V targets it is possible to limit the coproduction of the ^{46}Sc by using the energy range 35–19 MeV. The theoretical $^{47/46}$Sc production estimates based on the experimental results and the well-known DOTA-folate conjugate cm10 ([^{47}Sc]-cm10) biodistribution, allowed to evaluate the dose increase due to the presence of the ^{46}Sc contaminant [75]. The calculations showed that for E_p < 35 MeV and specific irradiation conditions considered, the effective Dose Increase (DI) due to the presence of contaminants was maintained within the 10% limit required for clinical use [75, 76]. However, to limit the presence of the ^{46}Sc contaminant, the calculated ^{47}Sc yield in the 35–19 MeV energy range is rather low, i.e. 0.1 GBq (irradiation conditions: 1 μA proton beams and 24 h of irradiation time), still suitable for preclinical studies [75].

Regarding the indirect reactions induced by protons to obtain the ^{47}Ca → ^{47}Sc precursor system, only few data are available in the international database [40]. The ^{51}V(p,x)^{47}Ca cross section was measured up to 250 MeV with a maximum value of about 0.2 mb making this route unfeasible [69]. No experimental data are present for the ^{50}Ti(p,x)^{47}Ca and the ^{49}Ti(p,x)^{47}Ca nuclear reactions, whose threshold energies are 24.5 and 21.2 MeV, respectively. On the other hand, the trend of the ^{48}Ca(p,x)^{47}Ca cross section was measured up to 19 MeV in 2019 [69], showing a maximum value of about 240 mb at 17 MeV. The low natural abundance of the target material (0.187%) has to be reminded that would make this route very expensive.

Considering the deuteron-induced reactions to produce ^{47}Sc, the:

- ^{nat}Ti(d,x)^{47}Sc excitation function has been measured by several authors [77–84], showing a good agreement in the increasing trend of the reaction cross section from low energy up to 50 MeV. Also the co-production of ^{46}Sc has been measured by different research teams and it is not possible to indicate a deuteron energy range where there is a pure ^{47}Sc production [77–86].
- ^{50}Ti(d,αn)^{47}Sc cross section was measured in 1964 [87], showing an increasing trend up to about 65 mb at 17.5 MeV; unfortunately, there are no data on the coproduction of ^{46}Sc, whose production threshold energy is 4.6 MeV.
- ^{49}Ti(d,α)^{47}Sc excitation function was measured in the same experimental campaign in 1964 [87], depicting a peak of about 45 mb at around 10 MeV. In this case, the ^{46}Sc coproduction was measured in the same energy range (7–20 MeV), obtaining an increasing trend with a plateau value of about 25 mb from 17.5 MeV up to 20 MeV; the lowest ^{49}Ti(d,αn)^{46}Sc cross section value is at 12 MeV, amounting to ca. 7 mb.
- ^{48}Ti(d,x)^{47}Sc cross section has never been measured (E_{thr} = 6.2 MeV). In the 1960s the ^{48}Ti(d,α)^{46}Sc excitation function was measured by different authors [87–89], giving a peak of 40 mb at around 12 MeV. It can be noted that there is a large discrepancy in the low energy region, around 7 MeV, with the value reported by Hall et al. [89] very close to 0 mb and the value measured by Chen et al. [87] around 24 mb; considering the agreement in the values reported by Chen et al. and Anders et al. [88], one may conclude that the 24 mb value is more reliable.
- ^{47}Ti(d,2p)^{47}Sc excitation function was also measured in 1964 by Chen et al. [87], showing an increasing trend from 10 MeV up to 20 MeV, with a maximum value of ca. 45 mb. There are no data regarding the ^{46}Sc coproduction, whose threshold energy is 5.2 MeV.
- ^{48}Ca(d,3n)^{47}Sc and ^{46}Ca(d,n)^{47}Sc cross sections were not measured, and also not for ^{46}Sc coproduction; the threshold energies are respectively 11.4 and 22.5 MeV for ^{47}Sc and ^{46}Sc production with ^{48}Ca targets, 0 and 4.8 MeV in case of ^{46}Ca targets.
- ^{nat}V(d,x)^{47}Sc cross section has been measured up to 90 MeV by three research teams, with agreeing results [90–92]. The cross section starts at 25 MeV and it reaches the maximum value of about 30 mb at ca. 40 MeV, then it decreases to 20 mb at 60 MeV with almost a flat trend up to the maximum energy. Unfortunately, the co-production of ^{46}Sc can be avoided only for deuteron energies <30 MeV. Below 40 MeV there is a low co-production of ^{46}Sc, since its production cross section is still at 5 mb, but it rapidly increases up to about 50 mb at ca. 55 MeV, keeping a quite flat trend up to 90 MeV.

Regarding the indirect reactions induced by deuterons to obtain the ^{47}Ca, it is possible to irradiate ^{nat}V targets: however, the production cross section is quite low (<0.4 mb) in the entire 30–90 MeV energy range investigated [91, 92].

Considering the α-induced reactions, the:

- ^{44}Ca(α,p)^{47}Sc cross section has been measured up to 45 MeV reaching a maximum value for ^{47}Sc production of about 120 mb at 14 MeV [50]; the same author also measured the coproduction of ^{46}Sc, finding a peak of about 400 mb at around 25–30 MeV. Although the natural abundance of ^{44}Ca is only 2.086%, the advantage in the use of α-beams lies in the short range

of α particles in Ca targets, allowing the use of a limited amount of enriched ^{44}Ca target material, compared to the use of proton and deuteron beams. The work published by Minegishi et al. [93] also reports the ^{47}Sc yield of about 11 MBq at the end of preparation (approximately 1.5 h from the EOB), obtained by irradiating a [^{44}Ca]CaO (^{44}Ca = 97.0 atom%, ^{40}Ca = 2.89 atom%) target of 200 mg in the energy range 28→0 MeV at 10 eμA, for 2 h irradiation. To obtain pure ^{47}Sc it is necessary to take into account the expected large coproduction of ^{46}Sc, not reported in the work by Minegishi et al. [93].

– ^{46}Ca(α,t)^{47}Sc cross sections are not known [40]; the threshold energies are respectively 12.3 and 23.9 MeV for ^{47}Sc and ^{46}Sc production.

In conclusion, some charged-particle induced reactions need to be measured to verify if they are feasible as ^{47}Sc production routes, e.g. $^{48/49/50}$Ti(p,x)^{47}Sc, ^{47}Ca → ^{47}Sc, $^{47/48/49/50}$Ti(d,x)^{47}Sc, ^{46}Ca/^{48}Ca(d,x)^{47}Sc and ^{46}Ca(α,x). From all the data available it turns out that the only ways to get ^{47}Sc without ^{46}Sc using light charged particle induced reactions lead to low production yield, not suitable for clinical use. It is thus necessary to study how to add a mass separation step to remove ^{46}Sc. Also in this case further cross section measurements will be needed to identify a precise impurity profile associated with each possible production route and it will be necessary to carefully look at mass separation technique, presumably coupled to laser ionization to be able to extract pure ^{47}Sc with high efficiency [94, 95].

2.3 ^{89}Zr

Thanks to its nuclear characteristics ($T_{1/2}$ = 78.41 h, 22.3% positron emission with a maximum energy of 900 keV), zirconium-89 (^{89}Zr) is a very promising radionuclide for immuno-PET [96]. Different experimental results obtained to produce zirconium-89 from a ^{89}Y target [97] may be compared by using both proton and deuteron beams [50]. The proton thick target yield is higher up to 26.5 MeV leading to higher production yield, whereas above 26.5 MeV the achievable yield with protons is lower than that obtained with deuterons [96, 98]. At the same time, a lower amount of radionuclidic impurities is produced by deuteron irradiation. For example, to keep a radionuclidic purity of 99.9%, it is possible to use a higher beam energy for deuterons (20.5 MeV) than for protons (16.2 MeV) which turns out in about 10% higher production yield for deuteron.

It is also possible to investigate other routes, such as the reactions ^{87,88}Sr(α,xn)^{89}Zr [50] that can be the object of further investigation as they seem competitive in the production of ^{89}Zr with possibly high radionuclidic purity.

2.4 ^{103}Pd

^{103}Pd ($T_{1/2}$ = 16.991 d) decays almost exclusively (99.90%) by electron capture (EC) to ^{103m}Rh ($T_{1/2}$ = 56.12 min) which de-excites through internal transition (IT) [36]. As a result of these processes (EC and IT) Auger-electrons and X-rays are emitted which are ideally suited for cancer therapy. Considering also the de-excitation of the "daughter" nuclide ^{103m}Rh, every 100 decays of ^{103}Pd are accompanied by the emission of about 263 Auger electrons, 188 low-energy conversion electrons and 97 X-rays. A comparison between the IAEA curve for the deuteron production and the IAEA curve for the proton production of ^{103}Pd [99] shows that the yields are comparable up to 12 MeV. For higher particle energies the achievable thick-target yield with deuterons is higher.

There are only two works reporting the production of ^{103}Pd by particles other than protons and deuterons [100–102]. Some of these reactions, mainly ^{101}Ru(α,2n)^{103}Pd and ^{103}Rh(^{3}He,x)^{103}Pd, may be worth the effort for further investigation in order to evaluate the achievable specific activity and the radionuclidic purities.

2.5 ^{186g}Re

^{186g}Re is a β^-/γ emitter radionuclide with a half-life of 90.64 h. The β^- end-point energies of 1.07 and 0.93 MeV suggest that this radionuclide is a good candidate for therapy of cancers with small tumour dimensions (from few millimetres to a few centimetres) [103]. Moreover, its γ-emission at 137.15 keV (very close to that of ^{99m}Tc) is in the energy range suitable for SPECT imaging (i.e., sufficiently high energy to penetrate the body and sufficiently low to be collimated by thin collimators and detected by thin detectors) [41, 42].

Very high specific activity ^{186g}Re can be produced by either proton [104–109] or deuteron [77, 110–116] cyclotron irradiation [117], provided an enriched target is used. It is possible to compare the experimental results obtained to produce rhenium-186g from a ^{nat}W target using proton and deuteron beams. The cross section values for the deuteron beams are considerably greater than for the proton beams. The maximum value that is possible to obtain with deuterons is almost 9 times greater than the maximum value

for the protons. This effect is also confirmed by the study of thick target yield [118]. It is possible to compare the integrated thin target yields of ^{186g}Re by using proton or deuteron beam: the two curves are coincident till energy of almost 8 MeV. From this energy up to 9 MeV, the yield of the proton bombardment is slightly larger than the deuteron one but starting from 9 MeV the deuteron yield grows much faster than that of the proton irradiation.

Even if there is a very short energy range in which proton irradiation is competitive with the deuteron one, there is no reason to prefer proton beams. In fact, the advantage of using deuterons over protons for the preparation of ^{186g}Re is double: more ^{186g}Re is formed and less ^{186}W is needed for the target, due to larger -dE/dx in the case of deuterons, by a factor of 4. This lower amount of target material is advantageous both to lower production cost and to simplify the dissolution of the target and its separation from the produced ^{186g}Re, with advantages also for waste and radioprotection purposes. This makes the deuteron route at facilities with medium-size cyclotrons the best choice for ^{186g}Re production.

It is also possible to investigate other routes [119–121] among which the ^{192}Os(p,α3n)^{186g}Re [119] and ^{186}W(α,x)^{186g}Re [120, 121] reactions may be of some interest. However, there is a high probability that other rhenium isotopes are produced and will affect the specific activity and the radionuclidic purity of the final product.

2.6 ^{97}Ru

The radionuclide ^{97}Ru, with a half-life of $T_{1/2}$ = 2.83 d, emits low-energy high-intensity γ lines (215.7 keV with 85.8% intensity and 324.5 keV with 10.8%) which have favourable characteristics for SPECT imaging. This can be beneficial to select a patient that may respond to new chemotherapy agents developed with ruthenium [122]. It decays by electron capture (EC) leading to Auger emission that can be used for Auger therapy. It can form a theranostic matched pair with ^{103}Ru ($T_{1/2}$ = 39.26 d) that decays to the short-lived Auger emitter ^{103m}Rh ($T_{1/2}$ = 56.12 min), a promising γ-free therapeutic agent.

Production of ^{97}Ru can be done by irradiation of ^{99}Tc with protons [123]. Unfortunately, Tc as a radioelement ($T_{1/2}$ = 2.111·10^5 y) is not easily available and it requires a dedicated infrastructure to be used as target material. Other reactions with proton-beams can be measured [124–126], but it seems more attractive to explore the use of an α particle beam coupled to a molybdenum target that is easily available as natural molybdenum or as enriched material [127–129]. Recently, new cross section values

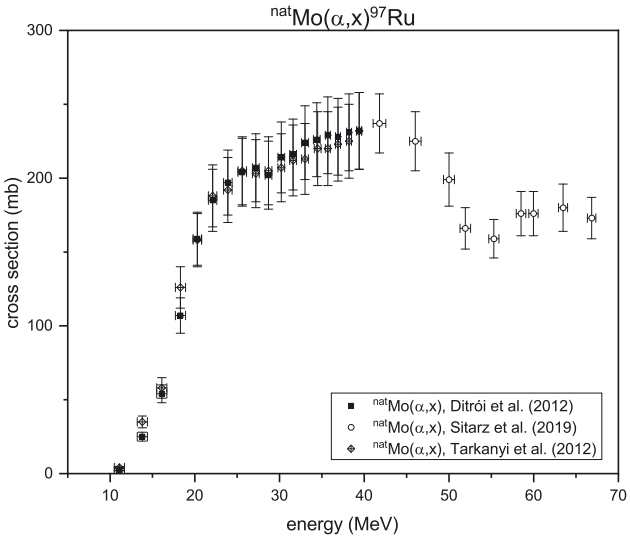

Figure 3: Measured cross section for ^{nat}Mo(α,x)^{97}Ru reaction [130] compared with data available in the literature [40, 131, 132].

[130] were measured toward higher energy in coherence with commercially available cyclotrons [15] which are able to deliver α-beam up to 70 MeV. These data allow the optimization of ^{nat}Mo(α,x)^{97}Ru production route and constrain the nuclear codes to explore the possibility to use enriched Mo targets. Figure 3 shows recent data reported in the literature for the cross sections of ^{nat}Mo(α,x) reactions to produce ^{97}Ru [123, 130–132].

A plateau is reached above 20 MeV coming from the fact that ^{nat}Mo is a mixture of six stable isotopes with comparable abundance. If enriched ^{95}Mo or ^{96}Mo targets are used instead, one can increase the production by a factor of five–six thanks to the natural abundances of these isotopes, that are respectively 15.84 and 16.67%, and considering that the beam energy can be defined adequately to favour the (α,2n) and (α,3n) reactions. Using a ^{nat}Mo target with a thickness of 100 mg/cm^2 and a 30 MeV beam energy, 3.5 MBq/μAh can be obtained. This example shows the benefit of having an α beam to allow for an alternative route when the target material is not easily available (see also [14]).

2.7 ^{211}At

^{211}At (Z = 85) is an α emitter that is promising for targeted α therapy. It has a half-life $T_{1/2}$ = 7.214 h and it emits one α particle per decay, either directly decaying to ^{207}Bi (41.80%, Eα = 5.869 MeV) or indirectly through EC (58.2%) to ^{211}Po, that quickly ($T_{1/2}$ = 0.516 s) decays to ^{207}Pb (E_α = 7.3695 MeV). In the emitted radiation by ^{211}At there are

also X-rays that can be used for imaging purpose. As the heavier stable element in the radionuclide chart is ^{209}Bi (Z = 83) and there is no long lived radionuclide in the close vicinity of ^{211}At, it is not possible to use low or medium energy proton or deuteron beams to produce it. The only possibility is to rely on an α particles beam impinging on a bismuth target (Z = 83). Bismuth is by chance monoisotopic, which makes target fabrication not expensive and easy to manufacture by evaporation under vacuum.

The energy threshold for ^{211}At production through the (α,2n) reaction is 20.7 MeV. In Figure 4, the family curves of integrated thick target Yields Y(E,ΔE) and the loci of the maxima, corresponding to optimal irradiation conditions for production, are presented. From these curves, it is clear that increasing the incident energy allows increasing the ^{211}At production. Unfortunately, ^{210}At ($T_{1/2}$ = 8.1 h) can also be produced by irradiation of a bismuth target with an alpha beam starting at 28.613 MeV (energy threshold of this reaction). This radionuclide must be avoided as much as possible, as it decays to the bone seeker ^{210}Po ($T_{1/2}$ = 138 d) that decays by α emission and it is highly radiotoxic. One possibility is to restrict the beam energy below the energy threshold of ^{210}At production but this will limit the production yield of ^{211}At at the same time. The rise of the ^{210}At production cross section is slow and there is room to optimize the irradiation parameters if one can define the acceptable limit of ^{210}At in the final ^{211}At product. This point is of fairly high importance as beam delivered by accelerators have some energy dispersion. In Table 4 the measured ^{210}At/^{211}At activity ratio are presented [133–135], showing how the ratio evolves as a function of the beam energy close to ^{210}At production energy threshold. From these data, it is clear how the choice of an incident energy of 28.8 MeV, slightly higher than the threshold energy (28.613 MeV) for the ^{209}Bi(α,3n)^{210}At reaction, allows to produce limited quantities of the ^{210}At radionuclide impurity, remaining below 1%, considered as a limit value.

More precise cross section values close to the ^{210}At threshold may help optimize production yield as a function of ^{211}At purity. In parallel, some toxicology studies on the impact of ^{210}At content in the final ^{211}At product are needed to get a consensus on the acceptable level of ^{210}At for medical application.

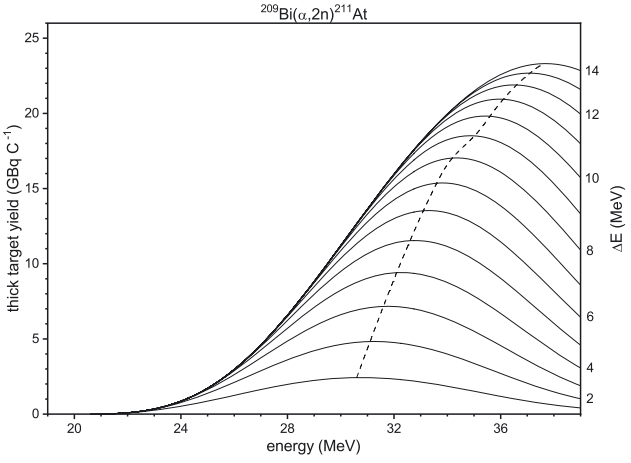

Figure 4: Integrated thick target yield for ^{211}At as a function of energy and energy loss into the target, with the loci of maxima corresponding to the couples (E,ΔE) for optimal irradiation conditions to produce the radionuclide with higher as possible yield, radionuclidic purity and specific activity [134].

3 Discussion and conclusion

Through the radionuclides discussed in this review (^{67}Cu, ^{47}Sc, ^{89}Zr, ^{103}Pd, ^{186g}Re, ^{97}Ru, ^{211}At) it has been high-lighted how the accelerated beam type and/or its energy and/or the target material have a direct impact on the production yield, the purity and the contaminants profile of the final product to be used for radiopharmaceuticals labelling procedure. Since the quality of the final product strongly depends on the chosen target/projectile/energy parameters set, the accurate knowledge of the production cross section of the desired radionuclide and related contaminants is the key point for the irradiation parameters optimization. Considering the frequently need of using isotope-enriched materials to limit as much as possible the coproduction of contaminants, the possibility to recover and reuse the irradiated target materials is an additional key aspect for the economical sustainability of the production cycle. For this reason, it is also useful to study the coproduction of radioactive isotopes (especially the long-lived ones) that may affect the recovery process.

An interesting example of this work is the ^{67}Cu case, whose production is usually based on the well-known

Table 4: Experimental activity ^{210}At/^{211}At ratio [134].

Beam energy (MeV)	27.6	28.6	28.8[a]	29.1	29.6	30.1	32.8[a]
^{210}At/^{211}At (%)	<4.4E-4	<0.01	0.001	0.023	0.18	0.7	7.4

The data ([a]) are reported in [134, 135].

(p,2p) reaction on ^{68}Zn targets; however, the high-energy ^{70}Zn(p,x)^{67}Cu route seems to be an interesting option and even a favourable route above 56 MeV, not only for the higher ^{67}Cu production yield (almost double), but also for the lower ^{64}Cu coproduction. From a practical point of view, it has to be outlined that the price of the enriched ^{68}Zn and ^{70}Zn material differs by a factor of about four, considering that the natural abundances of these zinc isotopes are 18.45 and 0.61%, respectively. The expenses of the enriched $^{68/70}$Zn isotopes can be amortised considering the possibility to recover and reuse the irradiated material, to manufacture new targets for a defined number of production cycles. In this case, it is important to know the production cross sections of the long-lived ^{65}Zn isotope (243.93 d half-life), to properly define the methods for the recovery process considering the activation of the material, minimizing as much as possible the dose imparted to the operator. With the development of high-energy high-intensity deuteron beams, the ^{70}Zn(d,x) production route will become attractive as it allows to obtain high-purity ^{67}Cu, as provided through the use of e-LINAC exploiting the ^{68}Zn(γ,x)^{67}Cu reaction [65].

As previously shown, the use of deuteron beams instead of the proton ones can sometimes be more effective (as for examples the ^{103}Pd and ^{186}Re case) or lead to a different impurity profile (e.g. the ^{67}Cu and ^{89}Zr cases). The criticality of these production routes is linked to the practical availability of accelerators with deuteron beams providing beam energies larger than 9 MeV and reasonable intensity (≥50 μA). On the other hand, considering radionuclides with a mid half-life as for the ^{186g}Re (3.7186 d) and ^{89}Zr (78.41 h) cases, nothing prevents to produce in centralized facilities with medium-size cyclotrons and ship them to the clinical centres over long distances. Also the increasing availability of intense α-beams may allow to bypass the limitations occurring when using protons or deuterons: this is the case of ^{97}Ru and ^{211}At production, and the possibility to investigate the new route for ^{186g}Re based on the ^{186}W(α,x)^{186g}Re cross section. On the other hand, also considering proton beams some interesting production routes have still to be investigated: as examples it can be reminded the ^{47}Sc production and the use of enriched Ti-targets, such as ^{49}Ti and ^{50}Ti.

A paradigmatic case is linked to the supply of the medically relevant Tb-isotopes, i.e. ^{149}Tb, ^{152}Tb, ^{155}Tb and ^{161}Tb [66]. These isotopes can be produced with different projectile/target/energy ranges, obtaining different yields and contaminant profiles; among the possible nuclear reactions to be exploited, some of them have still to be investigated. For the ^{155}Tb case [136–142], the main routes are based on the ^{155}Gd(p,n) and ^{156}Gd(p,2n) reactions, as outlined by a recent work [143], finding a purer ^{155}Tb with the (p,n) reaction and a higher yield with the (p,2n) one. On the other hand, ^{155}Tb can be also produced with a ^{155}Dy→^{155}Tb precursor system, exploiting the ^{155}Dy decay (9.9 h half-life). In this case, ^{155}Dy can be produced with high-energy proton beams and natural Tb-targets, using the ^{159}Tb(p,5n)^{155}Dy reaction [138, 144, 145]. Particular attention has to be paid to the coproduction of Dy-isotopes that decay to Tb and that may affect the final ^{155}Tb purity: the irradiation, decay, separation and elution times have thus to be carefully studied to maximize the ^{155}Tb radionuclidic purity. The advantage of the ^{159}Tb(p,5n)^{155}Dy→^{155}Tb route relies on the use of natural targets, even if the separation and purification chemistry among lanthanides is known to be challenging. The therapeutic ^{161}Tb is instead produced in nuclear reactors, exploiting the ^{160}Gd(n,γ)^{161}Gd→^{161}Tb route. Considering the charged particles induced reactions [136, 139, 140, 146], only deuterons can be competitive via the ^{160}Gd(d,x)^{161}Tb route (with a cross section of about 200 mb at ca. 10–15 MeV) [146], while the use of α-beams is possible, but curtailed by scarce availability and the low production yield of the ^{nat}Gd(α,x)^{161}Tb reaction [140]. The ^{149}Tb radionuclide, under the spotlight of the international community as α-emitter, can be produced with high-energy protons [147, 148]: in this case the coproduction of Tb-isotopes cannot be avoided, requiring the use of a mass separation method (either on-line or off-line) to select the desired radionuclide. The ^{152}Tb case is interesting since it is possible to compare the cross sections measured using proton, deuteron and α-beams on ^{151}Eu and ^{nat}Gd targets [137, 142, 147]. A promising production route may be the ^{nat}Gd(d,x)^{152}Tb reaction, that was measured up to 50 MeV obtaining an increasing trend with the maximum value of ca. 100 mb; however, the coproduction of contaminants has to be carefully evaluated. As for the ^{47}Sc case, it is particularly useful for the Tb-isotopes to take into account the possibility to use the mass separation method, as proposed by the ISOLDE-MEDICIS collaboration [94] and the PRISMAP consortium [95], to maximize the production yield and the final radionuclidic purity.

Reliable nuclear codes are useful tools to describe the production of the radionuclides difficult to be measured (such as stable isotopes, long-lived or short-lived radionuclides, etc.) and to evaluate their impact on the final product quality. Most of the available nuclear codes reproduce quite well the low-energy region of proton induced reactions. However, in the estimation of more exotic reactions induced by either high-energy protons or heavier projectiles (such as deuteron and α particles) there is room for improvements. This is also partly due to the scarce availability of experimental data to constrain the

nuclear codes in these regimes, another indication that further investigations are needed.

Considering the future availability of multi-particle accelerators and high-intensity beams, possibly coupled to mass separation techniques, it is foreseen that precise and complete set of cross section measurements will be needed to identify the best production route for the radionuclides of interest.

Author contribution: All the authors have accepted responsibility for the entire content of this submitted manuscript and approved submission.

Research funding: The National Institute of Nuclear Physics (INFN) of Italy has funded these research activities in the mainframe of projects approved by Interdisciplinary National Scientific Commission five since the eighties. The LARAMED project is funded by the Italian Ministry of Education, Universities and Research and it is based at the INFN Legnaro National Laboratories. The cyclotron Arronax is supported by CNRS, Inserm, INCa, the Nantes University, the Regional Council of Pays de la Loire, local authorities, the French government and the European Union. This work has been, in part, supported by a grant from the French National Agency for Research called "Investissements d'Avenir", Equipex Arronax-Plus noANR-11-EQPX-0004, Labex IRON noANR-11-LABX-18-01 and ISITE NExT no ANR-16-IDEX-007.

Conflict of interest statement: The authors declare no conflicts of interest regarding this article.

Employment or leadership: None declared.

Honorarium: None declared.

References

1. 2016-2022 World Nuclear Association, registered in England and Wales, number 01215741. Registered office: Tower House, 10 Southampton Street, London, WC2E 7HA, United Kingdom. *Radioisotopes in medicine|nuclear medicine*. https://world-nuclear.org/information-library/non-power-nuclear-applications/radioisotopes-research/radioisotopes-in-medicine.aspx.
2. Qaim S. M. *Medical Radionuclide Production, Science and Technology*; De Gruyter: Berlin/Boston, 2020.
3. Qaim S.M. Nuclear data relevant to cyclotron produced short-lived medical radioisotopes. *Radiochim. Acta* 1982, *30*, 147.
4. Qaim S. M. Theranostic radionuclides: recent advances in production methodologies. *J. Radioanal. Nucl. Chem.* 2019, *322*, 1257.
5. Qaim S. M., Scholten B., Neumaier B. New developments in the production of theranostic pairs of radionuclides. *J. Radioanal. Nucl. Chem.* 2018, *318*, 1493.
6. Herzog H., Rösch F., Stöcklin G., Lueders C., Qaim S. M., Feinendegen L. E. Measurement of pharmacokinetics of yttrium-86 radiopharmaceuticals with PET and radiation dose calculation of analogous yttrium-90 radiotherapeutics. *J. Nucl. Med.* 1993, *34*, 2222.
7. Srivastava S. A bridge not too far: personalized medicine with the use of theragnostic radiopharmaceuticals. *J. Postgrad. Med. Educ. Res.* 2013, *47*, 31.
8. Qaim S. M. Nuclear data for production and medical application of radionuclides: present status and future needs. *Nucl. Med. Biol.* 2017, *44*, 31.
9. Qaim S. M., Hussain M., Spahn I., Neumaier B. Continuing nuclear data research for production of accelerator-based novel radionuclides for medical use: a mini-review. *Front. Phys.* 2021, *9*, 639290.
10. Merrick M. J., Rotsch D. A., Tiwari A., Nolen J., Brossard T., Song J., Wadas T. J., Sunderland J. J., Graves S. A. Imaging and dosimetric characteristics of ^{67}Cu. *Phys. Med. Biol.* 2021, *66*, 035002.
11. Loveless C. S., Radford L. L., Ferran S. J., Queern S. L., Shepherd M. R., Lapi S. E. Photonuclear production, chemistry, and in vitro evaluation of the theranostic radionuclide ^{47}Sc. *EJNMMI Res.* 2019, *9*, 42.
12. Kazakov A. G., Ekatova T. Y., Babenya J. S. Photonuclear production of medical radiometals: a review of experimental studies. *J. Radioanal. Nucl. Chem.* 2021, *328*, 493.
13. IAEA. Cyclotron produced radionuclides: principles and practice. *Technical Reports Series No* 2008, *465*. https://www.iaea.org/publications/7849/cyclotron-produced-radionuclides-principles-and-practice.
14. Qaim S. M., Spahn I., Scholten B., Neumaier B. Uses of alpha particles, especially in nuclear reaction studies and medical radionuclide production. *Radiochim. Acta* 2016, *104*, 601.
15. Haddad F., Ferrer L., Guertin A., Carlier T., Michel N., Barbet J., Chatal J.-F. ARRONAX, a high-energy and high-intensity cyclotron for nuclear medicine. *Eur. J. Nucl. Med. Mol. Imag.* 2008, *35*, 1377.
16. Esposito J., Bettoni D., Boschi A., Calderolla M., Cisternino S., Fiorentini G., Keppel G., Martini P., Maggiore M., Mou L., Pasquali M., Pranovi L., Pupillo G., Rossi Alvarez C., Sarchiapone L., Sciacca G., Skliarova H., Favaron P., Lombardi A., Antonini P., Duatti A. LARAMED: a laboratory for radioisotopes of medical interest. *Molecules* 2019, *24*, 20.
17. IAEA. Cyclotron produced radionuclides: physical characteristics and production methods. 2009, https://www-pub.iaea.org/mtcd/publications/pdf/trs468_web.pdf.
18. Groppi F., Bonardi L. M., Bonardi L., Alfassi Z. B. Preparation of radionuclides and their measurement by high resolution γ-spectrometry, β-spectrometry and high resolution α-spectrometry. In *NATO Science for Peace and Security Series B: Physics and Biophysics*, 2009.
19. Koning A. J., Akkermans J. M. Pre-equilibrium nuclear reactions: an introduction to classical and quantum-mechanical models. In *Proceedings of the Workshop: Nuclear reaction data and nuclear reactors*; World Scientific: Singapore, 1999; pp. 143–158.
20. Goriely S., Hilaire S., Koning A. J. *Improved Predictions of Nuclear Reaction Rates with the TALYS Reaction Code for Astrophysical Applications*; Astronomy & Astrophysics, 487, 2008; p. 767.
21. Koning A. J., Rochman D. Modern nuclear data evaluation with the TALYS code system. *Nucl. Data Sheets* 2012, *113*, 2841.

22. Herman M., Capote R., Carlson B. V., Obložinský P., Sin M., Trkov A., Wienke H., Zerkin V. EMPIRE: nuclear reaction model code system for data evaluation. *Nucl. Data Sheets* 2007, *108*, 2655.
23. Böhlen T. T., Cerutti F., Chin M. P. W., Fassò A., Ferrari A., Ortega P. G., Mairani A., Sala P. R., Smirnov G., Vlachoudis V. The FLUKA code: developments and challenges for high energy and medical applications. *Nucl. Data Sheets* 2014, *120*, 211.
24. Ferrari A., Sala P. R., Fasso A., Ranft J. *FLUKA: A Multi-Particle Transport Code*; SLAC National Accelerator Lab: Menlo Park, CA (United States), 2005.
25. Pelowitz D. B., Durkee J. W., Elson J. S., Fensin M. L., Hendricks J. S., James M. R., Johns R. C., McKinney G. W., Mashnik S. G., Verbeke J. S., Waters L. S., Wilcox T. A. MCNPX 2.7.0 extensions. 2011. https://mcnp.lanl.gov/pdf_files/la-ur-11-02295.pdf.
26. Koning A. ISOTOPIA-1.0: simulation of medical isotope production with accelerators. 2019. https://nds.iaea.org/relnsd/isotopia/isotopia.pdf.
27. TENDL-2021 nuclear data library. https://tendl.web.psi.ch/tendl_2021/tendl2021.html.
28. Barbaro F., Canton L., Carante M. P., Colombi A., De Dominicis L., Fontana A., Haddad F., Mou L., Pupillo G. New results on proton-induced reactions on vanadium for ^{47}Sc production and the impact of level densities on theoretical cross sections. *Phys. Rev. C* 2021, *104*, 044619.
29. Synowiecki M. A., Perk L. R., Nijsen J. F. W. Production of novel diagnostic radionuclides in small medical cyclotrons. *Eur. J. Nucl. Med. Mol. I* 2018, *3*, 3.
30. Gales S. SPIRAL2 at GANIL: next generation of ISOL facility for intense secondary radioactive ion beams. *Nucl. Phys.* 2010, *834*, 717c.
31. Pichoff N., Bredy P., Ferrand G., Girardot P., Gougnaud F., Jacquemet M., Mosnier A., Bertrand P., Di Giacomo M., Ferdinand R., Berkovits D., Luner J., Rodnizki J. The SARAF-LINAC Project for SARAF-PHASE 2. In *6th International Particle Accelerator Conference (IPAC2015)*; JACoW Publishing: Richmond, VA, USA, 2015; pp. 3683–3685.
32. Alliot C., Audouin N., Barbet J., Bonraisin A.-C., Bossé V., Bourdeau C., Bourgeois M., Duchemin C., Guertin A., Haddad F., Huclier-Markai S., Kerdjoudj R., Laizé J., Métivier V., Michel N., Mokili M., Pageau M., Vidal A. Is there an interest to use deuteron beams to produce non-conventional radionuclides? *Front. Med.* 2015, *2*, 1–7.
33. Šimečková E., Bém P., Honusek M., Štefánik M., Fischer U., Simakov S. P., Forrest R. A., Koning A. J., Sublet J.-C., Avrigeanu M., Roman F. L., Avrigeanu V. Low and medium energy deuteron-induced reactions on ^{63,65}Cu nuclei. *Phys. Rev. C* 2011, *84*, 014605.
34. Baron N., Cohen B. L. Activation cross-section survey of deuteron-induced reactions. *Phys. Rev.* 1963, *129*, 2636.
35. Avrigeanu M., Avrigeanu V., Mănăilescu C. On reaction mechanisms involved in the deuteron-induced surrogate reactions. *AIP Conference Proceedings* 2015, *1645*, 139.
36. National Nuclear Data Center (NNDC) at Brookhaven National Laboratory. *NuDat*, *3*. https://www.nndc.bnl.gov/nudat3/.
37. Charged-particle cross section database for medical radioisotope production and beam monitor reactions. https://www-nds.iaea.org/medical/.
38. IAEA. Nuclear data for the production of therapeutic radionuclides. 2011. https://www-nds.iaea.org/publications/tecdocs/technical-reports-series-473.pdf.
39. Engle J. W., Ignatyuk A. V., Capote R., Carlson B. V., Hermanne A., Kellett M. A., Kibédi T., Kim G., Kondev F. G., Hussain M., Lebeda O., Luca A., Nagai Y., Naik H., Nichols A. L., Nortier F. M., Suryanarayana S. V., Takács S., Tárkányi F. T., Verpelli M. Recommended nuclear data for the production of selected therapeutic radionuclides. *Nucl. Data Sheets* 2019, *155*, 56.
40. NDS, IAEA, Experimental nuclear reaction data (EXFOR). https://www-nds.iaea.org/exfor/exfor.htm.
41. NDS, IAEA. Therapeutic radiopharmaceuticals labelled with copper-67, rhenium-186 and scandium-47. 2021. https://www.iaea.org/publications/14793/therapeutic-radiopharmaceuticals-labelled-with-copper-67-rhenium-186-and-scandium-47.
42. Jalilian A. R., Gizawy M. A., Alliot C., Takacs S., Chakarborty S., Rovais M. R. A., Pupillo G., Nagatsu K., Park J. H., Khandaker M. U., Mikolajczak R., Bilewicz A., Okarvi S., Gagnon K., Al Rayyes A. H., Lapi S. E., Starovoitova V., Korde A., Osso J. A. IAEA activities on ^{67}Cu, ^{186}Re, ^{47}Sc theranostic radionuclides and radiopharmaceuticals. *Curr. Rad.* 2021, *14*, 306.
43. Aslam M., Sudár S., Hussain M., Malik A. A., Shah H. A., Qaim S. M. Charged particle induced reaction cross section data for production of the emerging medically important positron emitter ^{64}Cu: a comprehensive evaluation. *Radiochim. Acta* 2009, *97*, 669.
44. Bonardi M. L., Groppi F., Mainardi H. S., Kokhanyuk V. M., Lapshina E. V., Mebel M. V., Zhuikov B. L. Cross section studies on ^{64}Cu with zinc target in the proton energy range from 141 down to 31 MeV. *J. Radioanal. Nucl. Chem.* 2005, *264*, 101.
45. Mou L., Martini P., Pupillo G., Cieszykowska I., Cutler C. S., Mikołajczak R. ^{67}Cu production capabilities: a mini review. *Molecules* 2022, *27*, 1501.
46. Qaim S. M. The present and future of medical radionuclide production. *Radiochim. Acta* 2012, *100*, 635.
47. De Nardo L., Pupillo G., Mou L., Esposito J., Rosato A., Meléndez-Alafort L. A feasibility study of the therapeutic application of a mixture of $^{67/64}$Cu radioisotopes produced by cyclotrons with proton irradiation. *Med. Phys.* 2022, *49*, 2709–2724.
48. Szelecsényi F., Steyn G. F., Dolley S. G., Kovács Z., Vermeulen C., van der Walt T. Investigation of the ^{68}Zn(p,2p)^{67}Cu nuclear reaction: new measurements up to 40 MeV and compilation up to 100 MeV. *Nucl. Instrum. Methods Phys. Res., Sect. B* 2009, *267*, 1877.
49. Stoll T., Kastleiner S., Shubin Y. N., Coenen H. H., Qaim S. M. Excitation functions of proton induced reactions on ^{68}Zn from threshold up to 71 MeV, with specific reference to the production of ^{67}Cu. *Radiochim. Acta* 2002, *90*, 309.
50. Levkovski V. N. *Cross Sections of Medium Mass Nuclide Activation (A=40-100) by Medium Energy Protons and Alpha-Particles (E=10-50 MeV)*; Intervesy: Moscow, USSR, 1991.
51. McGee T., Rao C., Saha G., Yaffe L. Nuclear interactions of ^{45}Sc and ^{68}Zn with protons of medium energy. *Nucl. Phys.* 1970, *A150*, 11–29.
52. Morrison D. L., Caretto A. A. Recoil study of the Zn^{68}(p,2p)Cu^{67} reaction. *Phys. Rev.* 1964, *133*, B1165.
53. Cohen B. L., Newman E., Handley T. H. (p,pn)+(p,2n) and (p,2p) cross sections in medium weight elements. *Phys. Rev.* 1955, *99*, 723.

54. Pupillo G., Sounalet T., Michel N., Mou L., Esposito J., Haddad F. New production cross sections for the theranostic radionuclide ^{67}Cu. *Nucl. Instrum. Methods Phys. Res., Sect. B* 2018, *415*, 41.
55. Kastleiner S., Coenen H. H., Qaim S. M. Possibility of production of ^{67}Cu at a small-sized cyclotron via the (p,α)-reaction on enriched ^{70}Zn. *Radiochim. Acta* 1999, *84*, 107.
56. Pupillo G., Mou L., Martini P., Pasquali M., Boschi A., Cicoria G., Duatti A., Haddad F., Esposito J. Production of ^{67}Cu by enriched ^{70}Zn targets: first measurements of formation cross sections of ^{67}Cu, ^{64}Cu, ^{67}Ga, ^{66}Ga, ^{69m}Zn and ^{65}Zn in interactions of ^{70}Zn with protons above 45 MeV. *Radiochim. Acta* 2020, *108*, 593.
57. Kozempel J., Abbas K., Simonelli F., Bulgheroni A., Holzwarth U., Gibson N. Preparation of ^{67}Cu via deuteron irradiation of ^{70}Zn. *Radiochim. Acta* 2012, *100*, 419.
58. Nigron E., Guertin A., Haddad F., Sounalet T. Is ^{70}Zn(d, x)^{67}Cu the best way to produce ^{67}Cu for medical applications? *Front. Med.* 2021, *8*, 674617.
59. Skakun Ye., Qaim S. M. Excitation function of the ^{64}Ni(α,p)^{67}Cu reaction for production of ^{67}Cu. *Appl. Radiat. Isot.* 2004, *60*, 33.
60. Tanaka S. Reactions of nickel with alpha-particles. *J. Phys. Soc. Jpn.* 1960, *15*, 2159.
61. Takács S., Aikawa M., Haba H., Komori Y., Ditrói F., Szűcs Z., Saito M., Murata T., Sakaguchi M., Ukon N. Cross sections of alpha-particle induced reactions on natNi: production of ^{67}Cu. *Nucl. Instrum. Methods Phys. Res., Sect. B* 2020, *479*, 125.
62. Antropov A. E., Zarubin P. P., Aleksandrov Y. A., Gorshkov I. Y. Study of the cross section for the reactions (p, n), (α,pn), (α,xn) on medium weight nuclei. *Presented at the Conf. Nucl. Spectr. and Nucl. Struct., Leningrad, USSR* 1985, 369.
63. Ohya T., Nagatsu K., Suzuki H., Fukada M., Minegishi K., Hanyu M., Zhang M.-R. Small-scale production of ^{67}Cu for a preclinical study via the ^{64}Ni(α,p)^{67}Cu channel. *Nucl. Med. Biol.* 2018, *59*, 56.
64. NIDC: National Isotope Development Center. https://isotopes.gov/.
65. Merrick M. J., Rotsch D. A., Tiwari A., Nolen J., Brossard T., Song J., Wadas T. J., Sunderland J., Graves S. Imaging and dosimetric characteristics of ^{67}Cu. *Phys. Med. Biol.* 2020, *66*, 035002.
66. Müller C., Domnanich K. A., Umbricht C. A., van der Meulen N. P. Scandium and terbium radionuclides for radiotheranostics: current state of development towards clinical application. *Br. J. Radiol.* 2018, *91*, 20180074.
67. Gadioli E., Gadioli Erba E., Hogan J. J., Burns K. I. Emission of alpha particles in the interaction of 10 85 MeV protons with ^{48,50}Ti. *Z. Phys. A-Hadron. Nucl.* 1981, *301*, 289.
68. Pupillo G., Fontana A., Canton L., Haddad F., Skliarova H., Cisternino S., Martini P., Pasquali M., Boschi A., Esposito J., Duatti A., Mou L. Preliminary results of the PASTA project. *Il Nuovo Cimento C* 2019, *42*, 1.
69. Carzaniga T. S., Braccini S. Cross-section measurement of ^{44m}Sc,^{47}Sc, ^{48}Sc and ^{47}Ca for an optimized ^{47}Sc production with an 18 MeV medical PET cyclotron. *Appl. Radiat. Isot.* 2019, *143*, 18.
70. Michel R., Peiffer F., Stück R. Measurement and hybrid model analysis of integral excitation functions for proton-induced reactions on vanadium, manganese and cobalt up to 200 MeV. *Nucl. Phys.* 1985, *441*, 617.
71. Michel R., Brinkmann G., Weigel H., Herr W. Measurement and hybrid-model analysis of proton-induced reactions with V, Fe and Co. *Nucl. Phys.* 1979, *322*, 40.
72. Ditrói F., Tárkányi F., Takács S., Hermanne A. Activation cross-sections of proton induced reactions on vanadium in the 37–65 MeV energy range. *Nucl. Instrum. Methods Phys. Res., Sect. B* 2016, *381*, 16.
73. Pupillo G., Mou L., Boschi A., Calzaferri S., Canton L., Cisternino S., De Dominicis L., Duatti A., Fontana A., Haddad F., Martini P., Pasquali M., Skliarova H., Esposito J. Production of ^{47}Sc with natural vanadium targets: results of the PASTA project. *J. Radioanal. Nucl. Chem.* 2019, *322*, 1711.
74. Pupillo G., Mou L., Boschi A., Calzaferri S., Canton L., Cisternino S., De Dominicis L., Duatti A., Fontana A., Haddad F., Martini P., Pasquali M., Skliarova H., Esposito J. Correction to: production of ^{47}Sc with natural vanadium targets: results of the PASTA project. *J. Radioanal. Nucl. Chem.* 2021, *328*, 1407.
75. Nardo L. D., Pupillo G., Mou L., Furlanetto D., Rosato A., Esposito J., Meléndez-Alafort L. Preliminary dosimetric analysis of DOTA-folate radiopharmaceutical radiolabelled with ^{47}Sc produced through ^{nat}V(p,x)^{47}Sc cyclotron irradiation. *Phys. Med. Biol.* 2021, *66*, 025003.
76. Meléndez-Alafort L., Ferro-Flores G., De Nardo L., Bello M., Paiusco M., Negri A., Zorz A., Uzunov N., Esposito J., Rosato A. Internal radiation dose assessment of radiopharmaceuticals prepared with cyclotron-produced ^{99m}Tc. *Med. Phys.* 2019, *46*, 1437.
77. Duchemin C., Guertin A., Haddad F., Michel N., Métivier V. Cross section measurements of deuteron induced nuclear reactions on natural tungsten up to 34 MeV. *Appl. Radiat. Isot.* 2015, *97*, 52.
78. Gagnon K., Avila-Rodriguez M. A., Wilson J., McQuarrie S. A. Experimental deuteron cross section measurements using single natural titanium foils from 3 to 9 MeV with special reference to the production of ^{47}V and ^{51}Ti. *Nucl. Instrum. Methods Phys. Res., Sect. B* 2010, *268*, 1392.
79. Takács S., Király B., Tárkányi F., Hermanne A. Evaluated activation cross sections of longer-lived radionuclides produced by deuteron induced reactions on natural titanium. *Nucl. Instrum. Methods Phys. Res., Sect. B* 2007, *262*, 7.
80. Hermanne A., Sonck M., Takács S., Tárkányi F. Experimental study of excitation functions for some reactions induced by deuterons (10–50 MeV) on natural Fe and Ti. *Nucl. Instrum. Methods Phys. Res., Sect. B* 2000, *161–163*, 178.
81. Takácss S., Sonck M., Scholten B., Hermanne A., Tárkányi F. Excitation functions of deuteron induced nuclear reactions on ^{nat}Ti up to 20 MeV for monitoring deuteron beams. *Appl. Radiat. Isot.* 1997, *48*, 657.
82. Lebeda O., Štursa J., Ráliš J. Experimental cross-sections of deuteron-induced reaction on ^{89}Y up to 20 MeV; comparison of ^{nat}Ti(d, x)^{48}V and ^{27}Al(d,x)^{24}Na monitor reactions. *Nucl. Instrum. Methods Phys. Res., Sect. B* 2015, *360*, 118.
83. Khandaker M. U., Haba H., Kanaya J., Otuka N. Excitation functions of (d,x) nuclear reactions on natural titanium up to 24 MeV. *Nucl. Instrum. Methods Phys. Res., Sect. B* 2013, *296*, 14.
84. Khandaker M. U., Haba H., Kanaya J., Otuka N., Kassim H. A. Activation cross-sections of deuteron-induced nuclear reactions on natural titanium. *Nucl. Data Sheets* 2014, *119*, 252.
85. Hermanne A., Tárkányi F., Takács S., Ditrói F., Amjed N. Excitation functions for production of ^{46}Sc by deuteron and

proton beams in ^{nat}Ti: a basis for additional monitor reactions. *Nucl. Instrum. Methods Phys. Res., Sect. B* 2014, *338*, 31.
86. Jung P. Helium production and long-term activation by protons and deuterons in metals for fusion reactor application. *J. Nucl. Mater.* 1987, *144*, 43.
87. Chen K. L., Miller J. M. Comparison between reactions of alpha particles with scandium-45 and deuterons with titanium-47. *Phys. Rev.* 1964, *134*, B1269.
88. Anders O. U., Meinke W. W. Absolute (d,α)-reaction cross sections of zirconium, molybdenum, titanium, and sulfur. *Phys. Rev.* 1960, *120*, 2114.
89. Hall K. L., Meinke W. W. Determination of (d,alpha) reaction cross-sections. *J. Inorg. Nucl. Chem.* 1959, *9*, 193–199.
90. Sonzogni A. A., Romo A. S. M. A., Mosca H. O., Nassiff S. J. Alpha and deuteron induced reactions on vanadium. *J. Radioanal. Nucl. Chem.* 1993, *170*, 143.
91. Qaim S. M., Probst H. J. Excitation functions of deuteron induced nuclear reactions on vanadium with special reference to the production of ^{43}K: systematics of (d,xn) reaction cross sections relevant to the formation of highly neutron deficient radioisotopes. *Radiochim. Acta* 1984, *35*, 11.
92. Tárkányi F., Ditrói F., Takács S., Hermanne A., Baba M., Ignatyuk A. V. Investigation of activation cross-sections of deuteron induced reactions on vanadium up to 40 MeV. *Nucl. Instrum. Methods Phys. Res., Sect. B* 2011, *269*, 1792.
93. Minegishi K., Nagatsu K., Fukada M., Suzuki H., Ohya T., Zhang M.-R. Production of scandium-43 and -47 from a powdery calcium oxide target via the nat/44Ca(α,x)-channel. *Appl. Radiat. Isot.* 2016, *116*, 8.
94. Duchemin C., Ramos J. P., Stora T., Ahmed E., Aubert E., Audouin N., Barbero E., Barozier V., Bernardes A.-P., Bertreix P., Boscher A., Bruchertseifer F., Catherall R., Chevallay E., Christodoulou P., Chrysalidis K., Cocolios T. E., Comte J., Crepieux B., Deschamps M., Dockx K., Dorsival A., Fedosseev V. N., Fernier P., Formento-Cavaier R., El Idrissi S., Ivanov P., Gadelshin V. M., Gilardoni S., Grenard J.-L., Haddad F., Heinke R., Juif B., Khalid U., Khan M., Köster U., Lambert L., Lilli G., Lunghi G., Marsh B. A., Palenzuela Y. M., Martins R., Marzari S., Menaa N., Michel N., Munos M., Pozzi F., Riccardi F., Riegert J., Riggaz N., Rinchet J.-Y., Rothe S., Russell B., Saury C., Schneider T., Stegemann S., Talip Z., Theis C., Thiboud J., van der Meulen N. P., van Stenis M., Vincke H., Vollaire J., Vuong N.-T., Webster B., Wendt K., Wilkins S. G. The CERN-MEDICIS collaboration: CERN-MEDICIS: a review since commissioning in 2017. *Front. Med.* 2021, *8*, 693682.
95. PRISMAP — building a European network for medical radionuclides. https://www.prismap.eu/.
96. Amjed N., Wajid A. M., Ahmad N., Ishaq M., Aslam M. N., Hussain M., Qaim S. M. Evaluation of nuclear reaction cross sections for optimization of production of the important non-standard positron emitting radionuclide ^{89}Zr using proton and deuteron induced reactions on ^{89}Y target. *Appl. Radiat. Isot.* 2020, *165*, 109338.
97. Cisternino S., Cazzola E., Skliarova H., Amico J., Malachini M., Gorgoni G., Anselmi-Tamburini U., Esposito J. Target manufacturing by spark plasma sintering for efficient ^{89}Zr production. *Nucl. Med. Biol.* 2022, *104–105*, 38.
98. Manenti S., Haddad F., Groppi F. New excitation functions measurement of nuclear reactions induced by deuteron beams on yttrium with particular reference to the production of ^{89}Zr. *Nucl. Instrum. Methods Phys. Res., Sect. B* 2019, *458*, 57.
99. IAEA. *Charged particle cross-section database for medical radioisotope production: diagnostic radioisotopes and monitor reactions* 2001, *IAEA-TECDOC-1211*. https://www-pub.iaea.org/MTCD/Publications/PDF/te_1211_prn.pdf.
100. Hussain M., Sudar S., Aslam M. N., Shah H. A., Ahmad R., Malik A. A., Qaim S. M. A comprehensive evaluation of charged-particle data for production of the therapeutic radionuclide ^{103}Pd. *Appl. Radiat. Isot.* 2009, *67*, 1842.
101. Ali B. M., Al-Abyad M., Kandil S., Solieman A. H. M., Ditrói F. Excitation functions of ^{3}He-particle-induced nuclear reactions on ^{103}Rh: experimental and theoretical investigations. *Eur. Phys. J. Plus.* 2018, *133*, 9.
102. Skakun Ye., Qaim S. M. Measurement of excitation functions of helion-induced reactions on enriched Ru targets for production of medically important ^{103}Pd and ^{101m}Rh and some other radionuclides. *Appl. Radiat. Isot.* 2008, *66*, 653.
103. Boschi A., Uccelli L., Pasquali M., Duatti A., Taibi A., Pupillo G., Esposito J. ^{188}W/^{188}Re generator system and its therapeutic applications. *J. Chem.* 2014, *2014*, 529406.
104. Tárkányi F., Takács S., Szelecsényi F., Ditrói F., Hermanne A., Sonck M. Excitation functions of proton induced nuclear reactions on natural tungsten up to 34 MeV. *Nucl. Instrum. Methods Phys. Res., Sect. B* 2006, *252*, 160.
105. Shigeta N., Matsuoka H., Osa A., Koizumi M., Izumo M., Kobayashi K., Hashimoto K., Sekine T., Lambrecht R. M. Production method of no-carrier-added ^{186}Re. *J Radioanal Nucl Ch* 1996, *205*, 85.
106. Zhang X., Li W., Fang K., He W., Sheng R., Ying D., Hu W. Excitation Functions for ^{nat}W(p,xn)$^{181-186}$Re Reactions and Production of No-Carrier-Added ^{186}Re via ^{186}W(p,n)^{186}Re Reaction. *Radiochim. Acta* 1999, *86*, 11.
107. Lapi S., Mills W. J., Wilson J., McQuarrie S., Publicover J., Schueller M., Schyler D., Ressler J. J., Ruth T. J. Production cross-sections of $^{181–186}$Re isotopes from proton bombardment of natural tungsten. *Appl. Radiat. Isot.* 2007, *65*, 345.
108. Khandaker M. U., Uddin M. S., Kim K., Lee M. W., Kim K. S., Lee Y. S., Kim G. N., Cho Y. S., Lee Y. O. Excitation functions of proton induced nuclear reactions on ^{nat}W up to 40 MeV. *Nucl. Instrum. Methods Phys. Res., Sect. B* 2008, *266*, 1021.
109. Bonardi M., Groppi F., Persico E., Manenti S., Abbas K., Holzwarth U., Simonelli F., Alfassi Z. B. Excitation functions and yields for cyclotron production of radiorhenium via ^{nat}W(p,†xn)$^{181-186g}$Re nuclear reactions and tests on the production of ^{186g}Re using enriched ^{186}W. *Radiochim. Acta* 2011, *99*, 1.
110. Manenti S., Persico E., Abbas K., Bonardi M. L., Gini L., Groppi F., Holzwarth U., Simonelli F. Excitation functions and yields for cyclotron production of radiorhenium via deuteron irradiation: ^{nat}W(d,xn)$^{181,182(A+B),183,184(m+g),186g}$Re nuclear reactions and tests on the production of ^{186g}Re using enriched ^{186}W. *Radiochim. Acta* 2014, *102*, 669.
111. Tárkányi F., Takács S., Szelecsényi F., Ditrói F., Hermanne A., Sonck M. Excitation functions of deuteron induced nuclear reactions on natural tungsten up to 50 MeV. *Nucl. Instrum. Methods Phys. Res., Sect. B* 2003, *211*, 319.

112. Nassiff S. J., Münzel H. Cross sections for the Reactions ^{66}Zn(d,n)^{67}Ga, ^{52}Cr(d,2n)^{52g}Mn and ^{186}W (d,2n)^{186}Re. *Radiochim. Acta* 1973, *19*, 97.
113. Pement F. W., Wolke R. L. Compound-statistical features of deuteron-induced reactions. ii. the compound nucleus and stripping-evaporation mechanisms in (d,2n) reactions. *Nucl. Phys.* 1966, *86*, 429–442.
114. Zhenlan T., Fuying Z., Huiyuan A. Q., Gongqing W. Excitation functions for $^{182\text{-}186}$W(d,2n)$^{182\text{-}186}$Re and ^{186}W(d,p)^{187}W reactions. *Chin. J. Nucl. Phys.* 1981, *3*, 242.
115. Ishioka N. S., Watanabe S., Osa A., Koizumi M., Matsuoka H., Sekine T. Excitation functions of rhenium isotopes on the ^{nat}W(d,xn) reactions and production of No-carrier-added ^{186}Re. *J. Nucl. Sci. Technol.* 2002, *39*, 1334.
116. Khandaker M. U., Nagatsu K., Minegishi K., Wakui T., Zhang M.-R., Otuka N. Study of deuteron-induced nuclear reactions on natural tungsten for the production of theranostic ^{186}Re via AVF cyclotron up to 38 MeV. *Nucl. Instrum. Methods Phys. Res., Sect. B* 2017, *403*, 51.
117. Hussain M., Sudár S., Aslam M. N., Malik A. A., Ahmad R., Qaim S. M. Evaluation of charged particle induced reaction cross section data for production of the important therapeutic radionuclide ^{186}Re. *Radiochim. Acta* 2010, *98*, 385.
118. Bonardi M. L., Groppi F., Manenti S., Persico E., Gini L. Production study of high specific activity NCA Re-186g by proton and deuteron cyclotron irradiation. *Appl. Radiat. Isot.* 2010, *68*, 1595.
119. Szelecsényi F., Steyn G. F., Kovács Z., Aardaneh K., Vermeulen C., van der Walt T. N. Production possibility of ^{186}Re via the ^{192}Os(p,α3n)^{186}Re nuclear reaction. *J. Radioanal. Nucl. Chem.* 2009, *282*, 261.
120. Scott N. E., Cobble J. W., Daly P. J. A comparison of reactions induced by medium-energy ^{3}He and ^{4}He ions in heavy target nuclei. *Nucl. Phys.* 1968, *119*, 131.
121. Aliev R. A., Zagryadskiy V. A., Kormazeva E. S., Latushkin S. T., Malamut T. Yu., Moiseeva A. N., Novikov V. I., Skobelin I. I., Unezhev V. N. Measurement of ^{186}W(^{4}He, p3n)^{186}Re, 186W(^{4}He, pn)^{188}Re, ^{186}W(4He,p)^{189}Re reaction cross sections by ^{4}He irradiation of ^{186}W target. *At. Energy* 2021, *130*, 36.
122. Lee S. Y., Kim C. Y., Nam T.-G. Ruthenium complexes as anticancer agents: a brief history and perspectives. *Drug Des. Dev. Ther.* 2020, *14*, 5375.
123. Zaitseva N. G., Rurarz E., Vobecký M., Hwan K. H., Nowak K., Téthal T., Khalkin V. A., Popinenkova L. M. Excitation function and yield for ^{97}Ru production in ^{99}Tc(p,3n)^{97}Ru reaction in 20 – 100 MeV proton energy range. In *Nuclear Data for Science and Technology*; Qaim S. M., Ed.; Springer: Berlin, Heidelberg, 1992; pp. 613–615.
124. Tárkányi F., Ditrói F., Takács S., Csikai J., Hermanne A., Uddin M. S., Baba M. Activation cross sections of proton induced nuclear reactions on palladium up to 80 MeV. *Appl. Radiat. Isot.* 2016, *114*, 128.
125. Uddin M. S., Hagiwara M., Baba M., Tarkanyi F., Ditroi F. Experimental studies on excitation functions of the proton-induced activation reactions on silver. *Appl. Radiat. Isot.* 2005, *62*, 533.
126. Ditrói F., Tárkányi F., Takács S., Mahunka I., Csikai J., Hermanne A., Uddin M. S., Hagiwara M., Baba M., Ido T., Shubin Yu., Dityuk A. I. Measurement of activation cross sections of the proton induced nuclear reactions on palladium. *J. Radioanal. Nucl. Chem.* 2007, *272*, 231.
127. Comparetto G., Qaim S. M. A comparative study of the production of short-lived neutron deficient isotopes ^{94,95,97}Ru in α- and ^{3}He-particle induced nuclear reactions on natural molybdenum. *Radiochim. Acta* 1980, *27*, 177.
128. Esterlund R. A., Pate B. D. Analysis of excitation functions via the compound statistical model: angular momentum effects. *Nucl. Phys.* 1965, *69*, 401.
129. Graf H. P., Münzel H. Excitation functions for α-particle reactions with molybdenum isotopes. *J. Inorg. Nucl. Chem.* 1974, *36*, 3647.
130. Sitarz M., Nigron E., Guertin A., Haddad F., Matulewicz T. New cross-sections for ^{nat}Mo(α,x) reactions and medical ^{97}Ru production estimations with radionuclide yield calculator. *Instruments* 2019, *3*, 7.
131. Ditrói F., Hermanne A., Tárkányi F., Takács S., Ignatyuk A. V. Investigation of the α-particle induced nuclear reactions on natural molybdenum. *Nucl. Instrum. Methods Phys. Res., Sect. B* 2012, *285*, 125.
132. Tárkányi F., Hermanne A., Ditrói F., Takács S., Ignatyuk A. Investigation of activation cross section data of alpha particle induced nuclear reaction on molybdenum up to 40 MeV: review of production routes of medically relevant ^{97,103}Ru. *Nucl. Instrum. Methods Phys. Res., Sect. B* 2017, *399*, 83.
133. Henriksen G., Messelt S., Olsen E., Larsen R. H. Optimisation of cyclotron production parameters for the ^{209}Bi(α,2n)^{211}At reaction related to biomedical use of ^{211}At. *Appl. Radiat. Isot.* 2001, *54*, 839.
134. Morzenti S., Bonardi M. L., Groppi F., Zona C., Persico E., Menapace E., Alfassi Z. B. Cyclotron production of ^{211}At/^{211g}Po by ^{209}Bi(α,2n) reaction. *J. Radioanal. Nucl. Chem.* 2008, *276*, 843.
135. Groppi F., Bonardi M. L., Birattari C., Menapace E., Abbas K., Holzwarth U., Alfarano A., Morzenti S., Zona C., Alfassi Z. B. Optimisation study of α-cyclotron production of At-211/Po-211g for high-LET metabolic radiotherapy purposes. *Appl. Radiat. Isot.* 2005, *63*, 621.
136. Tárkányi F., Ditrói F., Takács S., Csikai J., Hermanne A., Ignatyuk A. V. Activation cross-sections of long lived products of deuteron induced nuclear reactions on dysprosium up to 50 MeV. *Appl. Radiat. Isot.* 2014, *83*, 18.
137. Tárkányi F., Takács S., Ditrói F., Csikai J., Hermanne A., Ignatyuk A. V. Activation cross-sections of deuteron induced reactions on ^{nat}Gd up to 50 MeV. *Appl. Radiat. Isot.* 2014, *83*, 25.
138. Tárkányi F., Takács S., Ditrói F., Hermanne A., Ignatyuk A. V. Activation cross-sections of longer-lived radioisotopes of deuteron induced nuclear reactions on terbium up to 50 MeV. *Nucl. Instrum. Methods Phys. Res., Sect. B* 2013, *316*, 183.
139. Szelecsényi F., Kovács Z., Nagatsu K., Zhang M.-R., Suzuki K. Investigation of deuteron-induced reactions on ^{nat}Gd up to 30 MeV: possibility of production of medically relevant ^{155}Tb and ^{161}Tb radioisotopes. *J. Radioanal. Nucl. Chem.* 2016, *307*, 1877.
140. Gayoso R. E., Sonzogni A. A., Nassiff S. J. (α,pxn) reactions on natural gadolinium. *Radiochim. Acta* 1996, *72*, 55.
141. Mosca H. O., Capurro O., Vedoya M. V., Nassiff S Excitation functions and thick target yields of (α,αxn) and (α, 2pxn) reactions on ^{159}Tb. *J. Radioanal. Nucl. Chem.* 1989, *131*, 435–443.
142. Duchemin C., Guertin A., Haddad F., Michel N., Métivier V. Deuteron induced Tb-155 production, a theranostic isotope for SPECT imaging and auger therapy. *Appl. Radiat. Isot.* 2016, *118*, 281.

143. Favaretto C., Talip Z., Borgna F., Grundler P. V., Dellepiane G., Sommerhalder A., Zhang H., Schibli R., Braccini S., Müller C., van der Meulen N. P. Cyclotron production and radiochemical purification of terbium-155 for SPECT imaging. *Eur. J. Nucl. Med. Mol. I* 2021, *6*, 37.
144. Tárkányi F., Hermanne A., Ditrói F., Takács S., Ignatyuk A. V. Activation cross-sections of longer lived radioisotopes of proton induced nuclear reactions on terbium up to 65 MeV. *Appl. Radiat. Isot.* 2017, *127*, 7.
145. Engle J. W., Mashnik S. G., Parker L. A., Jackman K. R., Bitteker L. J., Ullmann J. L., Gulley M. S., Pillai C., John K. D., Birnbaum E. R., Nortier F. M. Nuclear excitation functions from 40 to 200 MeV proton irradiation of terbium. *Nucl. Instrum. Methods Phys. Res., Sect. B* 2016, *366*, 206.
146. Tárkányi F., Hermanne A., Takács S., Ditrói F., Csikai J., Ignatyuk A. V. Cross-section measurement of some deuteron induced reactions on ^{160}Gd for possible production of the therapeutic radionuclide ^{161}Tb. *J. Radioanal. Nucl. Chem.* 2013, *298*, 1385.
147. Moiseeva A. N., Aliev R. A., Unezhev V. N., Gustova N. S., Madumarov A. S., Aksenov N. V., Zagryadskiy V. A. Alpha particle induced reactions on ^{151}Eu: possibility of production of ^{152}Tb radioisotope for PET imaging. *Nucl. Instrum. Methods Phys. Res., Sect. B* 2021, *497*, 59.
148. Formento-Cavaier R., Haddad F., Alliot C., Sounalet T., Zahi I. New excitation functions for proton induced reactions on natural gadolinium up to 70 MeV with focus on ^{149}Tb production. *Nucl. Instrum. Methods Phys. Res., Sect. B* 2020, *478*, 174.